AEM
Journals.ASM.org

Formate Oxidation-Driven Calcium Carbonate Precipitation by *Methylocystis parvus* OBBP

Giovanni Ganendra,[a,e] Willem De Muynck,[a,b] Adrian Ho,[c] Eleni Charalampous Arvaniti,[b] Baharak Hosseinkhani,[a] Jose Angel Ramos,[d] Hubert Rahier,[d] Nico Boon[a]

Laboratory of Microbial Ecology and Technology, Ghent University, Ghent, Belgium[a]; Magnel Laboratory of Concrete Research, Ghent University, Ghent, Belgium[b]; Department of Microbial Ecology, Netherlands Institute of Ecology (NIOO-KNAW), Wageningen, The Netherlands[c]; Research Group Physical Chemistry and Polymer Science, Vrije Universiteit Brussel, Brussels, Belgium[d]; SIM vzw, Zwijnaarde, Belgium[e]

Microbially induced carbonate precipitation (MICP) applied in the construction industry poses several disadvantages such as ammonia release to the air and nitric acid production. An alternative MICP from calcium formate by *Methylocystis parvus* OBBP is presented here to overcome these disadvantages. To induce calcium carbonate precipitation, *M. parvus* was incubated at different calcium formate concentrations and starting culture densities. Up to 91.4% ± 1.6% of the initial calcium was precipitated in the methane-amended cultures compared to 35.1% ± 11.9% when methane was not added. Because the bacteria could only utilize methane for growth, higher culture densities and subsequently calcium removals were exhibited in the cultures when methane was added. A higher calcium carbonate precipitate yield was obtained when higher culture densities were used but not necessarily when more calcium formate was added. This was mainly due to salt inhibition of the bacterial activity at a high calcium formate concentration. A maximum 0.67 ± 0.03 g of $CaCO_3$ g of $Ca(CHOOH)_2^{-1}$ calcium carbonate precipitate yield was obtained when a culture of 10^9 cells ml^{-1} and 5 g of calcium formate $liter^{-1}$ were used. Compared to the current strategy employing biogenic urea degradation as the basis for MICP, our approach presents significant improvements in the environmental sustainability of the application in the construction industry.

Microbially induced carbonate precipitation (MICP) is a well-known process and has been extensively described in the past (1–3). In short, MICP produces carbonate minerals, e.g., calcium carbonate, as a result of alterations in environmental conditions. In nature, examples of MICP include calcite formation in soils (4), limestone caves (5), seas (6), and soda lakes (7). Four different key parameters that govern microbially induced calcium carbonate precipitation are the: (i) concentration of nonprecipitated calcium, (ii) concentration of the total inorganic carbon, (iii) pH, and (iv) availability of nucleation sites for calcium carbonate crystal formation (3). Among the four parameters, bacterial activities mainly influence the pH of the environment (1).

MICP is the basis for several biotechnological applications in the construction sector (for a review, see reference 1 and references therein). These include the use of calcium carbonate precipitate to protect concrete surface against the ingress of deleterious substances (e.g., chloride ions) (8) or to heal cracks in aging concrete (9, 10). Among the bacterial activities that can induce calcium carbonate precipitation, urea degradation by heterotrophic bacteria is typically used for applications on building materials. In biogenic urea degradation, urea is transformed to ammonia and carbonate ions to initiate precipitation (11). *Bacillus* spp. (e.g., *B. sphaericus*) is the most commonly applied urea degrader for MICP in the construction sector due to several advantages such as the high initial urea degradation rate by the strain and a highly negative ζ potential of the strain (12).

However, the use of urea degradation-based MICP in the construction sector poses several drawbacks. First, ammonia production can pollute the air. Second, with pKa of ammonium/ammonia around 9.25 at 25°C (13), ammonium can be present inside the building material and nitrified by the bacteria into nitric acid, which in turn reacts with calcite from the building material to form calcium nitrate. Calcium nitrate is a highly soluble component and the dissolution of this component in the building material can contribute to the biodeterioration of the material (14). Therefore, an alternative MICP for application in the construction sector needs to be investigated.

Methane-oxidizing bacteria (MOB) are a subset of methylotrophic bacteria capable of utilizing methane as their carbon and energy source (15). As part of the dissimilatory methane oxidation pathway, MOB oxidize formate to CO_2 using the formate dehydrogenase enzyme. *Methylocystis parvus* OBBP, a type II MOB, has been previously investigated for biotechnological applications. *M. parvus* OBBP is known to synthesize poly-3-hydroxybutyrate (PHB), a biopolymer that is used as a raw material for bioplastics (16). The strain accumulates PHB intracellularly when it is provided with an excess of carbon source and in the absence of sufficient essential nutrients (e.g., nitrogen, phosphorus, etc.) (16, 17). For bioremediation purposes, the particulate methane monooxygenase enzyme expressed by *Methylocystis* spp. can also degrade several pollutants such as halogenated alkanes (18, 19).

In this research, *M. parvus* OBBP is investigated as an alternative biocatalyst to induce calcium carbonate precipitation from calcium formate. We hypothesize that formate utilization by *M. parvus* OBBP will lead to an increase of pH and carbonate production. With the availability of calcium ions from calcium formate

Received 23 April 2014 **Accepted** 12 May 2014
Published ahead of print 16 May 2014
Editor: J. E. Kostka
Address correspondence to Nico Boon, Nico.Boon@UGent.be.
This publication is publication no. 5617 of the Netherlands Institute of Ecology.

doi:10.1128/AEM.01349-14

and the potential use of *M. parvus* OBBP cell wall as the nucleation site, calcium carbonate precipitation is favored. This study is divided into two parts. First, a proof of principle of calcium carbonate precipitation by *M. parvus* OBBP from calcium formate was performed. Second, the influence of the culture density and calcium formate concentration to the calcium carbonate precipitate yield was investigated.

MATERIALS AND METHODS

Bacterial strain and culture condition. *Methylocystis parvus* OBBP was obtained from Colin Murrell (School of Environmental Science, University of East Anglia). *M. parvus* OBBP was grown in nitrate mineral salt (NMS) medium (20) in serum bottles (Schott-Duran, USA) under an ~20% (vol/vol) methane mixing ratio in the headspace. The bottles were incubated on a shaker (120 rpm) at 28°C. For the precipitation experiments, 20-fold-lower phosphate buffer concentrations (i.e., 35.9 and 13.6 mg of $Na_2HPO_4 \cdot 12H_2O$ and KH_2PO_4 liter^{-1}, respectively) in the NMS medium were used. This was done to minimize the buffering capacity of the medium but for the medium to still sufficiently provide a phosphorus source for the bacterial growth. Experiments were performed using 125-ml PYREX serum bottles (Corning, USA). Bottles were acid washed by immersion in 1 M nitric acid (VWR, Belgium) for 1 day and left to dry to remove trace metals from the bottles' surface. Incubations were performed aseptically by autoclaving the bottles at 120°C for 20 min before experiments and by preparing the set up under laminar flow.

Calcium carbonate precipitation by *M. parvus* OBBP. This experiment was performed to investigate MICP from calcium formate by *M. parvus* OBBP. *M. parvus* OBBP was grown until mid-logarithmic phase before the cells were collected by centrifugation at 10,000 × *g* for 10 min, washed twice with saline solution (8.5 g of NaCl liter^{-1}), and resuspended in NMS medium. A 50-μl portion of the culture was sampled to determine the total number of cells before they were added into the serum bottles. Sterile calcium formate and NMS medium were mixed in different bottles (working volume, 7 ml) to have final formate concentrations of: 0.04, 0.14, 0.44, 0.72, 1.1, 1.44, 1.83, 2.32, and 2.88 g liter^{-1}. Then, 1 ml of the culture was added to each bottle. Serum bottles containing bacterial culture and NMS medium without formate addition served as a reference. Next, 2-ml portions of liquid sample were taken from each bottle, filtered using a 0.22-μm-pore-size filter (Millipore, USA), and stored at 4°C until further analysis. The bottles were then capped with butyl rubber stoppers (Rubber B.V., The Netherlands), sealed with crimp caps (Agilent Technologies, Belgium), and incubated on a shaker (120 rpm) at 28°C for 4 days, after which sampling was performed. Approximately 2 ml of liquid was taken at the end of incubation period from each bottle for bacterial cell counting and liquid sample analysis. After cell count determination, the liquid samples were filtered using a 0.22-μm-pore-size filter (Millipore) and stored at 4°C until further analysis.

The influence of methane addition on calcium carbonate precipitation by *M. parvus* OBBP was also investigated. Sealed serum bottles with bacterial inoculated mixture of calcium formate and NMS medium were injected with methane (99.5% [vol/vol]; Air Liquide, Belgium) to reach ~10% (vol/vol) methane mixing ratio in the headspace. Afterward, the headspace gas composition was determined, and the gas pressure was measured using a tensimeter (WIKA, Germany). This was repeated daily. Methane oxidation rate (MOR) by *M. parvus* OBBP was determined by linear regression after the methane depletion in the headspace over time. The liquid sampling procedure, as described previously, was done before and after the incubation.

For all types of incubations, reference incubations containing *M. parvus* OBBP in sodium formate and uninoculated calcium formate were performed. For both incubations, methane was added into the bottles. Incubations in sodium formate were done to investigate the evolution of measured parameters (e.g., bacterial growth) when calcium carbonate precipitation was absent. The uninoculated calcium formate incubations were performed to verify that the calcium carbonate precipitation was driven by the bacterial formate oxidation. Incubations were performed in triplicates. For simplification, the following symbols were assigned to the different treatments: bacterial incubations in methane and calcium formate (M1), calcium formate (M2), and methane and sodium formate (M3). M4 was assigned to the uninoculated incubations containing calcium formate under methane.

Optimization of calcium carbonate precipitate yield from calcium formate by *M. parvus* OBBP. This experiment was performed to determine the influence of calcium formate concentrations and bacterial cell densities to the calcium carbonate precipitation yield from calcium formate [g of $CaCO_3$ g of $Ca(CHOOH)_2^{-1}$]. Triplicate incubations from each of 10^6, 10^7, 10^8, and 10^9 *M. parvus* OBBP cells ml^{-1} and 0.5, 2.5, 5, and 10 g of calcium formate liter^{-1} were prepared. *M. parvus* OBBP was grown in NMS medium, and the cells were collected as described previously. The bacterial culture was resuspended in deionized water. For each treatment, an 8-ml mixture of sterile calcium formate and the bacterial culture was made in the serum bottles. Before and after the incubation, 2 ml of liquid sample was taken, filtered using a 0.22-μm-pore-size filter, and stored at 4°C until further analysis. The serum bottles were then capped with butyl rubber stoppers and incubated for 1 day on a shaker (120 rpm) at 28°C. In this experiment, methane was not added into the bottles. When the process is applied on building wall, to minimize bacterial washout due to environmental effects such as rain, then fast precipitation is preferred. Thus, a short incubation time was set in the experiment.

Additional 50-ml incubations of 10^9 *M. parvus* OBBP cells ml^{-1} without calcium formate addition and in 2.5, 5, and 10 g of calcium formate liter^{-1} were carried out. The bigger liquid volume was used in order to obtain a sufficient biomass pellet from the culture after the experiment. The pellets were used to determine calcium carbonate crystals morphology, phase, and polymorphs. The biomass pellets were collected after the experiments as described previously.

Bacterial cell count. Bacterial cell count was performed using a BD Accuri C6 flow cytometer (BD Biosciences, Belgium) according to the live/dead staining protocol described by Van Nevel et al. (21). For the analysis, each culture sample contains a 500-μl mixture of bacterial culture (5 or 50 μl, depending on the dilution factor), fluorescent dyes (5 μl; the dye composition is described in reference 22), and sterile physiological solution (0.9% [vol/vol] NaCl). The total number of propidium iodide- and SYBR green-tagged cells per ml of the analyzed sample was reported as the culture density.

Gas composition analysis. Methane and oxygen were measured by using a compact gas chromatograph (GC; Global Analyser Solution, The Netherlands) equipped with a thermal conductivity detector, a Porabond precolumn, and a Molsieve SA column. Then, 1 ml of gas sample was taken from each serum bottle before injection into the GC using a gas-tight syringe (Hamilton, Belgium).

Liquid sample analysis. Liquid samples were analyzed for (i) formate concentration, (ii) soluble calcium concentration, and (iii) pH. The formate concentrations in samples were measured by using DX-500 BioLC liquid chromatograph that was equipped with an AS1 column and an ED50 conductivity detector (Dionex, USA). The soluble calcium concentration was measured by using an AA-6300 atomic absorption spectrophotometer (Shimadzu, Japan). Portions (100 and 200 μl) of 65% (vol/vol) nitric acid (VWR, Belgium) and 1 g of lanthanium standard solution (Chem-Lab, Belgium) liter^{-1}, respectively, were added to each sample before analysis. The amount of calcium carbonate precipitated was calculated from the amount of the removed soluble calcium in the culture. The pH was measured using a C-532 pH electrode (Consort, Belgium).

XRD. Stored biomass pellets of an *M. parvus* OBBP culture of 10^9 cells ml^{-1} in 0, 2.5, 5, and 10 g of calcium formate liter^{-1} were used for the identification of the calcium carbonate precipitated crystal phase by X-ray diffractometry (XRD) analysis. XRD spectra for each sample was analyzed using a Thermo Scientific ARL X'TRA powder diffractometer equipped with a Peltier cooled detector. The X-ray diffractometer was operated at

40 kV and 30 mA with monochromated CuKα radiation. XRD data, over a range of 3 to 60° 2θ, were collected with a step size of 0.02° and a preset time of 1 s at each step.

SEM. Stored biomass pellets of an *M. parvus* OBBP culture of 10^9 cells ml^{-1} in 5 g of calcium formate $liter^{-1}$ were used for the scanning electron microscopy (SEM) analysis. The pellet was placed on an aluminum stub with a carbon conductive tab and dried at 60°C for approximately 2 h to remove the water content in the pellet. In addition to the image analysis, elemental composition analysis of the samples was also carried out using an energy-dispersive X-ray spectroscopy (EDS). SEM and EDS analysis were performed using a Phenom ProX desktop scanning electron microscope (Phenom-World BV, Eindhoven, The Netherlands), with 10- and 15-kV accelerating voltages for image and EDS analysis, respectively. Before analysis, samples were sputtered with a 2-nm Pt-Pd coating. Samples of nonbiogenic calcium carbonate were also analyzed by EDS and used as a reference.

TEM. Stored biomass pellets of an *M. parvus* OBBP culture of 10^9 cells ml^{-1} in 5 g of calcium formate $liter^{-1}$ were used for transmission electron microscopy (TEM) analysis. The bacteria were fixed in 0.1 M cacodylate buffer containing 4% paraformaldehyde and 5% glutaraldehyde. TEM images were collected at 50 kV using the method previously described by Hosseinkhani et al. (23). Images were obtained by using Zeiss TEM 900 transmission electron microscope using (Carl Zeiss, Germany).

Statistical analysis. Other than pH measurements, except as stated otherwise, values are means from triplicate measurements, and error bars represent standard deviations. pH measurements were carried out once for each type of incubation. Statistical analyses were done in SigmaPlot v12.0 (Systat Software, Inc., USA) to compare significant differences of values between different incubations by means of one-way analysis of variance test ($P = 0.05$).

RESULTS

Calcium carbonate precipitation by *M. parvus* OBBP from calcium formate. A 1- to 2-log increase in *M. parvus* OBBP culture densities was observed in almost all methane-amended cultures compared to their initial culture densities (Fig. 1a). However, for all type of incubations, lower culture densities were exhibited by the bacteria at formate concentrations higher than 1.44 g $liter^{-1}$. The MOR exhibited by *M. parvus* OBBP also decreased at higher formate concentrations (Fig. 1b). The bacteria showed a higher MOR in M1 than in M3 when the same amount of formate was added, except for 1.83 and 2.88 g of formate $liter^{-1}$, where the differences were not significant ($P > 0.05$).

M. parvus OBBP exhibited higher calcium removal in M1 than in M2 at formate concentrations higher than 0.5 g $liter^{-1}$ (Fig. 1c). In M1, it was observed that the bacterial calcium removal exhibited a hyperbolic increase from 3.5% ± 0.6% to 91.4% ± 1.6% at 0.04 and 2.88 g of formate $liter^{-1}$, respectively. *M. parvus* OBBP could not remove >50% of the initial calcium in M2 at all of the formate concentrations tested. The bacteria removed formate completely at different formate concentrations in M1, whereas various formate removals were exhibited by the bacteria in M2 or M3 (Fig. 1d). Decreasing formate removal was exhibited by the bacteria in M2 and M3 when a formate concentration higher than 1.5 g $liter^{-1}$ was added. In M2, *M. parvus* OBBP exhibited only a maximum of 61.7% ± 9.1% formate removal, and this was observed when 1.1 g of formate $liter^{-1}$ was added into the culture. The calcium and formate removal exhibited in all M4 incubations were not significant. An increase in pH in all cultures was observed when formate was added into the *M. parvus* OBBP culture (Table 1). A greater pH increase was observed in M3 when formate at >1.44 g $liter^{-1}$ was added. In M1 and M2, at concentrations of >0.44 mg of formate $liter^{-1}$, the pH changes in the cultures were not appreciable.

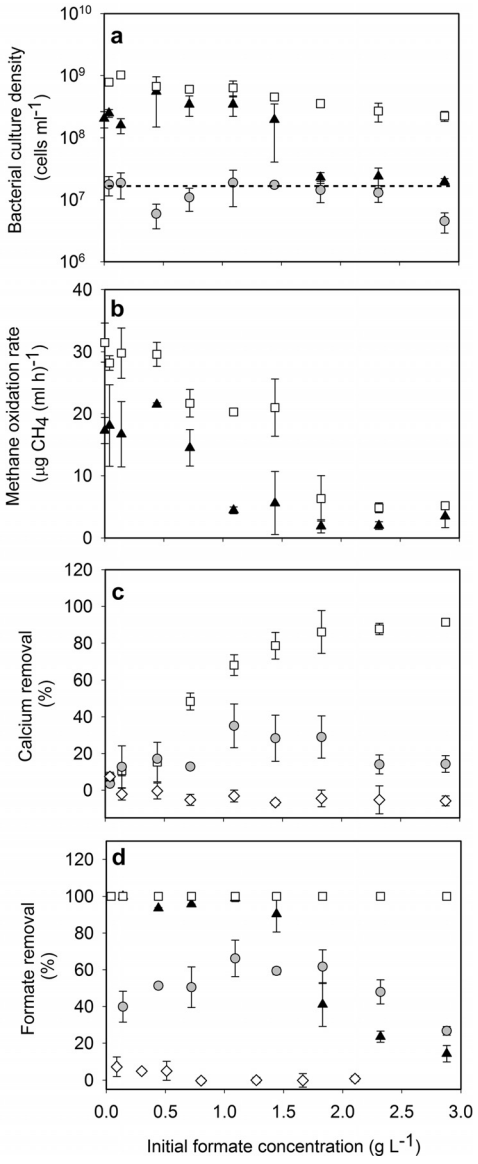

FIG 1 Culture density (a), methane oxidation rate (b), calcium removal (c), and formate removal (d) exhibited in M1 (open squares), M2 (gray-shaded circles), M3 (solid triangles), and M4 (open diamonds) incubations. The symbols represent different types of incubations: bacterial incubations in methane and calcium formate (M1), calcium formate (M2), and methane and sodium formate (M3). M4 was assigned to the uninoculated incubations containing calcium formate under methane. The dotted line in panel a indicates the initial *M. parvus* OBBP culture density (9×10^6 cells ml^{-1}). Values are the average of triplicate measurements. Error bars represent the standard deviations.

Influence of calcium formate concentration and bacterial cell density on the calcium carbonate precipitation yield. The calcium and formate removal of *M. parvus* OBBP was dependent on the calcium formate concentration and the culture density used (Table 2). At the same calcium formate concentration, higher calcium and formate removal was obtained in cultures when higher culture densities were used, the exception being bacterial calcium removal at 0.5 g of calcium formate $liter^{-1}$. However, using the same value of culture density, higher calcium and for-

TABLE 1 Initial pH and pH differences in M1, M2, and M3 cultures before and after incubation

Initial formate concn (g liter^{-1})	pH or dpH[a]					
	M1		M2		M3	
	pH	dpH	pH	dpH	pH	dpH
0	6.6	0	6.6	0	6.6	ND
0.04	6.6	0.8	6.6	0.4	6.4	0.9
0.14	6.6	1	6.6	0.9	6.5	1
0.44	6.7	1.2	6.7	1.2	6.6	1.0
0.72	6.8	1.1	6.8	1.3	6.7	1.1
1.10	6.9	1.1	6.9	1.1	6.7	1.2
1.44	6.9	1.1	6.9	1.3	ND	ND
1.83	6.9	1.1	6.9	1.2	6.7	1.8
2.32	6.8	1.3	6.8	1.2	6.8	1.6
2.88	6.7	1.2	6.7	1.2	6.8	1.3

[a] pH refers to the initial incubation pH (i.e., at $t = 0$) of the *M. parvus* OBBP culture. dpH is the pH increase in the *M. parvus* OBBP culture before and after the incubation period. ND, not determined.

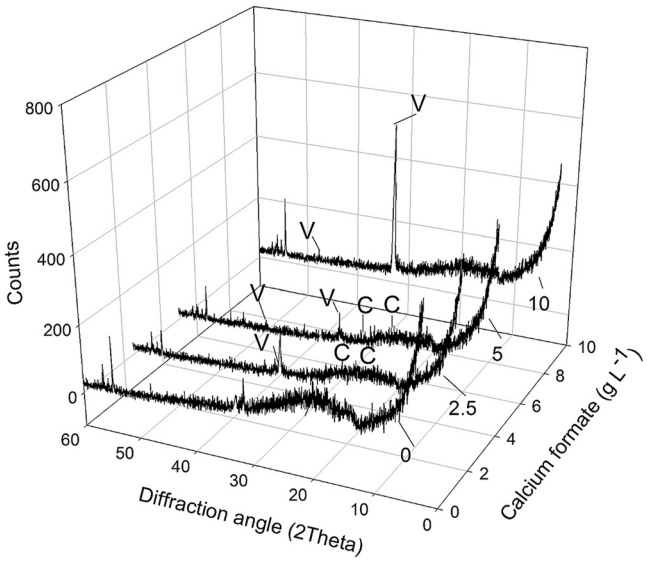

FIG 2 XRD pattern from the biomass pellets of *M. parvus* OBBP cultures in 0 (i.e., no calcium formate addition), 2.5, 5, and 10 g of calcium formate liter^{-1}. V and C indicate the XRD peaks that correlate with valerite and calcite peaks, respectively.

mate removal was not necessarily exhibited by bacteria when greater calcium formate concentrations were used. For example, in a culture of 10^9 cells ml^{-1}, less calcium and formate removal was observed in the cultures at 10 g of calcium formate liter^{-1} (36.7% ± 7.1% [formate] and 31.8% ± 5.6% [calcium]) than at 5 g liter^{-1} of calcium formate (98.5% ± 0.1% [formate] and 87.4% ± 3.8% [calcium]).

The maximum calcium carbonate precipitate yield obtained from different culture densities and calcium formate concentrations tested was 0.67 ± 0.03 g of $CaCO_3$ g of $Ca(CHOOH)_2^{-1}$ (Table 2). The yield was calculated from the amount of calcium carbonate precipitated (i.e., the removal of soluble calcium) over the amount of the calcium formate added. For each tested culture density, the maximum calcium carbonate precipitation yield could be obtained when 2.5 g of calcium formate liter^{-1} was added. The maximum calcium carbonate precipitation yield, as described previously, was obtained from 5 g of calcium formate liter^{-1} and cultures of 10^9 cells ml^{-1}. However, there was no significant yield difference when either 2.5 or 5 g of calcium formate liter^{-1} was added ($P > 0.05$).

Morphologies, polymorphs, and cellular locations of the calcium carbonate crystals produced by *M. parvus* OBBP. Vaterite and calcite were the two main polymorphs identified in the calcium carbonate crystals from *M. parvus* OBBP cultures at various formate concentrations (Fig. 2). Several peaks of vaterite and calcite polymorphs were depicted in almost all XRD spectra from each type of culture. The highest vaterite peak was significantly shown in the culture at 10 g of calcium formate liter^{-1}. The vaterite compositions in all incubations except at 5 g of formate liter^{-1} were between 80 to 90% (wt/wt), whereas the calcite composition at 5 g of formate liter^{-1} was 58.5% (wt/wt) (calculated data). Aragonite was also detected in crystals from all type of incubations with a maximum of 6.6% (wt/wt) in culture at 10 g of formate liter^{-1} (calculated data).

The morphologies and likely cellular locations of the bacterially induced calcium carbonate crystals are indicated in TEM and SEM images (Fig. 3 and Fig. 4). Calcium carbonate crystals seem to accumulate and adsorb on the surface of the bacterial cell wall (Fig. 3). This observation was seen in almost all bacterial cells in the TEM images. Spherical crystals shape were observed in bacterial cultures when 5 or 10 g of calcium formate liter^{-1} were added (Fig. 4). Grouped spherulite crystals were observed in an SEM image of the culture at 10 g of calcium formate liter^{-1} but not at 5 g of calcium formate liter^{-1}. The energy-dispersive spectra of the spherulite were similar to those of nonbiogenic calcium carbonate, whereas the mean peak of calcium (i.e., 3.69 keV) in the energy dispersive spectra at places without the spherical crystals were significantly lower.

TABLE 2 Formate removal, calcium removal, and calcium carbonate precipitation yield in cultures of *M. parvus* OBBP[a]

Calcium formate concn (g liter^{-1})	Mean formate removal, calcium removal, and calcium carbonate precipitation yields ± the SD at an *M. parvus* OBBP culture density cells ml^{-1} of:											
	10^6 cells ml^{-1}			10^7 cells ml^{-1}			10^8 cells ml^{-1}			10^9 cells ml^{-1}		
	Formate removal (%)	Calcium removal (%)	$CaCO_3$ yield	Formate removal (%)	Calcium removal (%)	$CaCO_3$ yield	Formate removal (%)	Calcium removal (%)	$CaCO_3$ yield	Formate removal (%)	Calcium removal (%)	$CaCO_3$ yield
0.5	5.8 ± 2.2	10.9 ± 1.9	0.08 ± 0.01	33.0 ± 1.4	7.2 ± 3.1	0.06 ± 0.02	100	5.1 ± 1.6	0.04 ± 0.01	100	5.5 ± 2.3	0.04 ± 0.02
2.5	0.7*	8.5*	0.07*	5.9 ± 1.6	19.8 ± 4.1	0.15 ± 0.03	67.2 ± 1.5	57.4 ± 3.5	0.44 ± 0.03	96.9 ± 0.1	82.1 ± 4.7	0.63 ± 0.04
5	1.4 ± 0.8	9.0 ± 2.1	0.07 ± 0.02	2.5 ± 1.9	9.0 ± 3.8	0.07 ± 0.03	34.0 ± 1.1	26.1 ± 2.6	0.20 ± 0.02	98.5 ± 0.1	87.4 ± 3.8	**0.67 ± 0.03**
10	0.7 ± 0.4	7.5 ± 4.1	0.06 ± 0.03	2.3 ± 0.5	4.6 ± 2.0	0.04 ± 0.02	10.2 ± 2.1	6.7 ± 2.6	0.05 ± 0.02	36.7 ± 7.1	31.8 ± 5.6	0.24 ± 0.04

[a] Formate removal, calcium removal, and calcium carbonate precipitation yields were determined in the cultures of *M. parvus* OBBP incubated at various culture densities and concentrations of calcium formate. Calcium carbonate ($CaCO_3$) yields are expressed as g of $CaCO_3$ g of $Ca(CHOOH)_2^{-1}$. The value in boldface indicates the maximum calcium carbonate precipitation yield obtained from the test. *, averages of duplicate measurements.

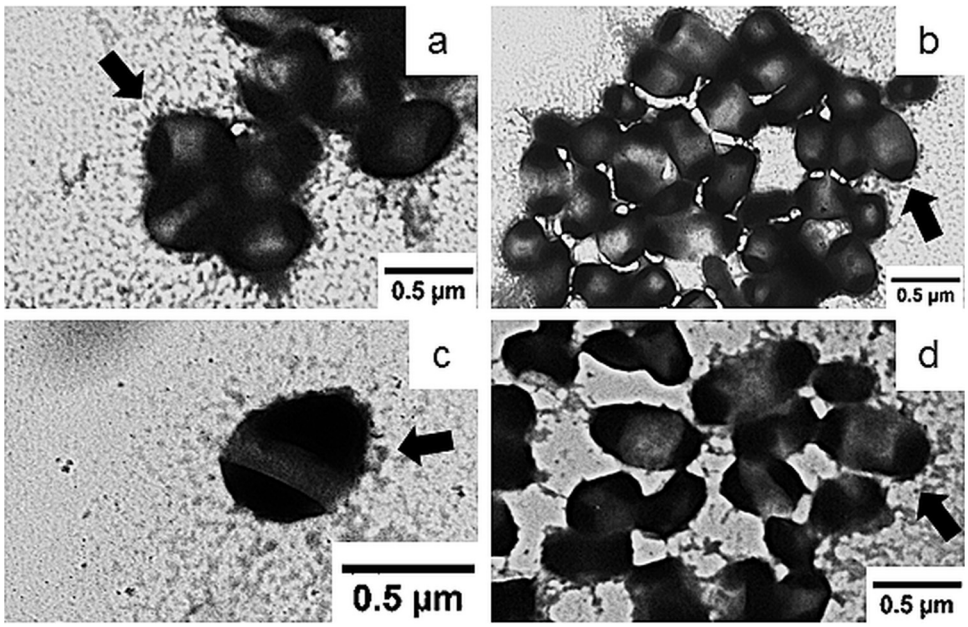

FIG 3 (a to d) TEM images of *M. parvus* OBBP cultures in 5 g of calcium formate liter^{-1}. The arrows indicate the likely locations of calcium carbonate crystals on the bacterial cells.

DISCUSSION

Calcium carbonate precipitation by *M. parvus* OBBP from calcium formate. Significant bacterial growth was only observed in the methane-amended cultures (Fig. 1a). This was due to the fact that biomass could only be synthesized by the bacteria from methane but not formate. Methane oxidation by *M. parvus* OBBP generates formaldehyde, an intermediate for carbon assimilation via the serine cycle (15). Formate transformation to CO_2 generates NADH that can only be used as a reducing power in other metabolic processes, for example, hydroxypyruvate conversion to glycerate in the serine cycle (24). Moreover, formate addition could inhibit *M. parvus* OBBP growth, as indicated by the lower MOR exhibited by the bacteria (Fig. 1b). From the Herbert-Pirt equation, a low specific substrate utilization rate results in a low specific biomass growth (25). In our study, the low MOR was likely caused by the low methane concentration in the liquid phase. From the hyperbolic substrate utilization kinetic (26), with methane as the sole carbon and energy source, MOB exhibited low MOR at a low methane concentration. The lower dissolved methane concentration upon formate addition was likely a consequence of the lower methane solubility; salt addition lowers the water potential and thus lowers the methane diffusivity into the liquid phase (27).

Without significant calcium and formate removal in M4, calcium carbonate precipitation occurred as a result of the bacterial formate oxidation (Fig. 1c and d). Formate conversion to CO_2 by *M. parvus* OBBP led to an increase of the pH in the culture (Table 1). Previous studies have shown that bacterial or fungal utilization of low molecular organic compounds such as formate (e.g., acetate) would lead to an increase in environmental pH (4, 28, 29). In a solution, formate and CO_2 are in equilibrium with formic acid and carbonic acid, respectively. The pH increase in the cultures occurred due to the bacterial conversion of formic acid to the weaker carbonic acid, and this would shift the carbonate system toward carbonate ions production (equation 1 [30]). Calcium carbonate was then formed from the reaction between calcium ions from calcium formate and carbonate ions from the formate conversion (equation 2).

$$CO_{2(g)} \leftrightarrow CO_{2(aq)} + H_2O \leftrightarrow H_2CO_3 \leftrightarrow H^+ + HCO_3^- \leftrightarrow H^+ + CO_3^- \quad (1)$$

$$Ca^{2+} + CO_3^{2-} \leftrightarrow CaCO_3 \quad (2)$$

$$\Omega = \frac{a(Ca^{2+})a(CO_3^{2-})}{K_{so}} \quad \text{with } K_{so\ \text{calcite, } 25^\circ C} = 3.8 \times 10^{-9}\ \text{mol liter}^{-1} \quad (3)$$

Based on the thermodynamic approach, when the total ionic activity product from the calcium carbonate formation exceeds the calcium carbonate equilibrium constant (K_{so}), then the system is supersaturated (i.e., saturation state [Ω] > 1), and calcium carbonate precipitation is likely to occur (see equation 3) (1).

Influence of calcium formate concentration and bacterial cell density on the calcium carbonate precipitation yield. Higher calcium carbonate precipitate yields were obtained when higher *M. parvus* OBBP culture densities were used but not necessarily at higher calcium formate concentrations (Table 2). At higher formate concentrations, the precipitation time, salt stress, and crystallization surface area availability were limiting the precipitation rate. A longer incubation time was needed for the substrate (e.g., formate) conversion to induce precipitation at a high substrate concentration (31). A higher formate and calcium removal exhibited by the bacteria are therefore anticipated at longer incubation times. A high calcium formate addition also increased the salt stress imposed on the cells, thus limiting their activity (18). *Methylocystis* spp. are generally known to be robust and able to withstand different forms of stress (18, 32, 33); however, *M. parvus* OBBP is not proven to be a halophilic MOB (20). Hence, the addition of salt may eventually inhibit the activity of the bacteria. The inhibition effect of calcium formate to the precipitation yield

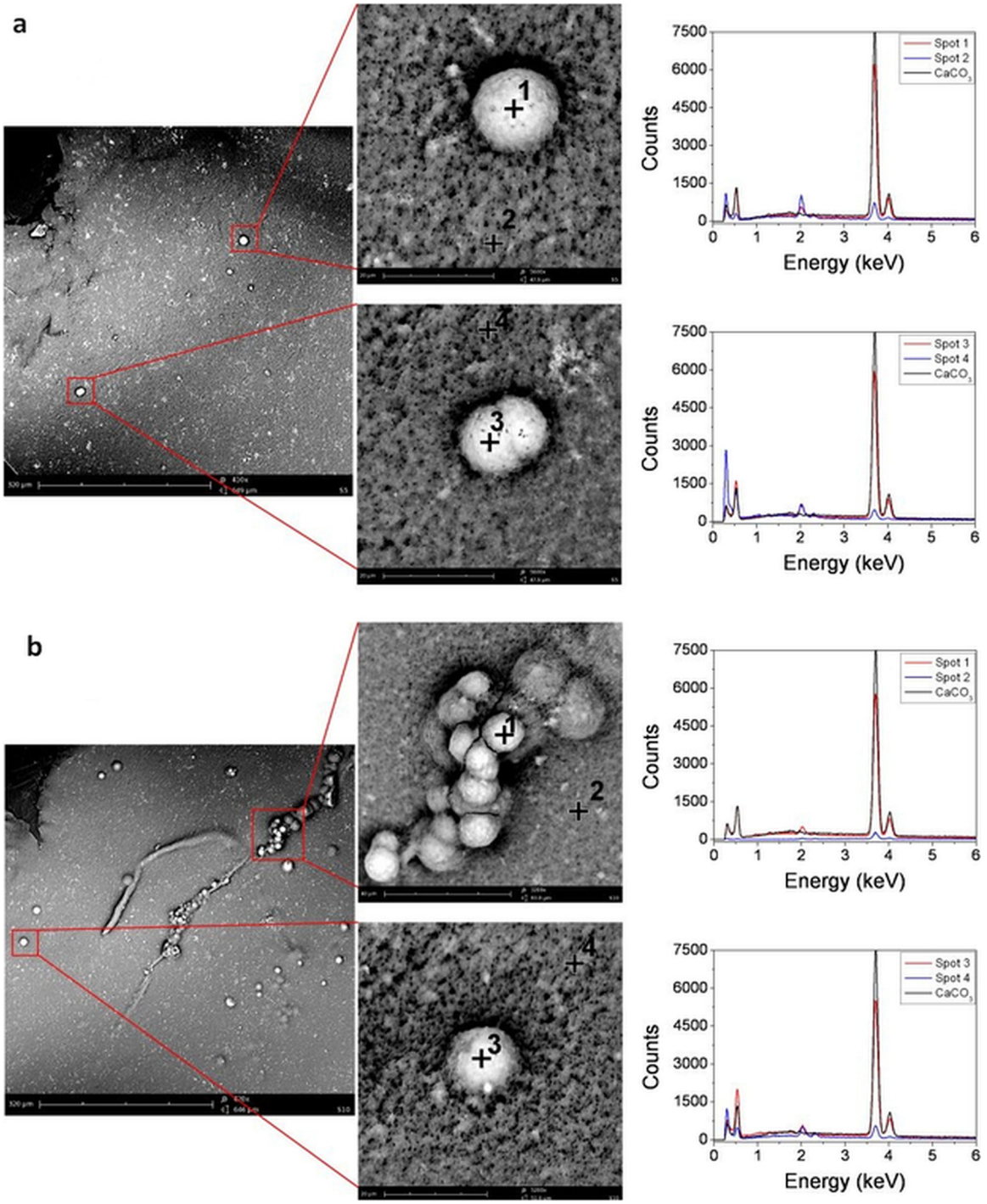

FIG 4 SEM images and EDS spectra of *M. parvus* OBBP culture in 5 g (a) or 10 g (b) of calcium formate liter^{-1}. EDS analyses were done at predicted calcium carbonate crystal spots (i.e., spots 1 and 3 [red line]) and at places without calcium carbonate crystals (i.e., spots 2 and 4 [blue line]). For reference, the EDS of nonbiogenic calcium carbonate crystals are also shown in the graph (black line).

was observed especially when 10 g of calcium formate liter^{-1} was added. Moreover, there was a limited surface area available for the bacteria to bind calcium ions for a given amount of biomass. Therefore, further addition of calcium formate did not necessarily result in a higher calcium carbonate precipitate yield. Overall, as observed in another study (34), there is an optimum process condition to obtain a maximum calcium carbonate precipitate yield. In our study, 5 g of calcium formate liter^{-1} and 10^9 cells ml^{-1} were the optimum calcium formate concentration and culture density, respectively, to obtain a maximum calcium carbonate precipitate yield.

On a per-cell basis, the optimum biomineralization rate ob-

TABLE 3 Comparison of calcium carbonate biomineralization rates obtained in this study with a urea-based approach

Strain	Biomineralization rate[a]			$CaCO_3$ crystal polymorph(s)	Biomineralization substrates[b]	Source or reference
	10^{-13} g Ca^{2+} (h cell)$^{-1}$	10^{-3} g Ca^{2+} (h OD)$^{-1}$	10^{-8} g Ca^{2+} (h CFU)$^{-1}$			
M. parvus OBBP	6.0 ± 0.4[c]			Calcite, vaterite, aragonite	$Ca(CHOOH)_2$ (5 g liter^{-1})	This study
B. pasteurii ATCC 6453	16			Calcite	Urea (3 g liter^{-1}) and $CaCl_2$ (2.8 g liter^{-1})	11, 35, 36
S. pasteurii ATCC 11859[d]	7.2			Calcite and vaterite	Urea (20 g liter^{-1}) and $CaCl_2$ (2.8 mg liter^{-1})	47–52
B. megaterium ATCC 10788	0.16*			Calcite and vaterite	Urea (20 g liter^{-1}) and $CaCl_2$ (2.8 g liter^{-1})[f]	53
B. megaterium AP6	0.83*			Calcite	Urea (20 g liter^{-1}) and $CaCl_2$ (2.8 g liter^{-1})	54
E. coli HB101[e]	13			Calcite	Urea (3 g liter^{-1}) and $CaCl_2$ (2 g liter^{-1})	52
E. ludwigii		33		Calcite and vaterite	Urea (20 g liter^{-1}) and $CaCl_2$ (18.8 g liter^{-1})	55
P. vulgaris		4.3			Urea (20 g liter^{-1}) and $CaCl_2$ (28.3 g liter^{-1})	56
S. soli KNUC401		23.8		Calcite	Urea (20 g liter^{-1}) and $CaCl_2$ (3.7 g liter^{-1})	57
B. massiliensis KNUC402		13.1		Calcite	Urea (20 g liter^{-1}) and $CaCl_2$ (3.7 g liter^{-1})	57
A. crystallopoietes KNUC403		13.9		Calcite	Urea (20 g liter^{-1}) and $CaCl_2$ (3.7 g liter^{-1})	57
L. fusiformis KNUC404		15.2		Calcite	Urea (20 g liter^{-1}) and $CaCl_2$ (3.7 g liter^{-1})	57
S. ginsegisoli CR5			5.4	Calcite, vaterite, aragonite	Urea (20 g liter^{-1}) and $CaCl_2$ (2.8 mg liter^{-1})	58
K. flava CR1			2.7	Calcite and aragonite	Urea (20 g liter^{-1}) and $CaCl_2$ (3.7 g liter^{-1})	59, 60

[a] The biomineralization rate is expressed as the soluble calcium removal rate in the bacterial culture. *, these two biomineralization rates were calculated assuming that the mass of one bacterium is 10^{-12} g.

[b] If several references are given for a specific strain, then the substrate composition and the biomineralization rate were taken from or calculated based on the first reference provided.

[c] This biomineralization rate value was taken from cultures that exhibited the highest calcium carbonate precipitation yield (5 g of calcium formate liter^{-1} and 10^9 cells ml^{-1}). The value is the average of triplicate measurements. The error value represents the standard deviation.

[d] Previously known as *Bacillus pasteurii* ATCC 11859.

[e] Plasmid pBU11 was constructed with the entire sequence of the urease gene cluster taken from *S. pasteurii* ATCC 11859.

[f] 35% (vol/vol) CO_2 was added in the headspace of the incubator.

tained from our study (i.e., at 5 g liter^{-1} calcium formate and 10^9 cells ml^{-1}) is still approximately three times lower than the maximum urea based biomineralization rate (*B. pasteurii* ATCC 6453; Table 3). *B. pasteurii* ATCC 6453 has also been applied in other areas of environmental biotechnology as the biocatalyst to remediate contaminated soils (35, 36). The urease-based MICP from *Bacillus* spp. was the focus of many studies because they are known to possess the urease gene and exhibit a high urea degradation rate (12, 37). Accordingly, the construction industry mostly utilized these strains for the MICP based biotechnological applications (e.g., concrete surface treatment and self-healing concrete) (1, 38, 39). The MICP of strains from other bacteria have also been studied but, the assessment of their biotechnological potential compare to our study is difficult as other studies used different units to express biomineralization rates (Table 3). For future study, an optimization in the biomineralization rate of the MICP based on calcium formate utilization by *M. parvus* OBBP should be conducted.

The morphologies, polymorphs, and cellular locations of the calcium carbonate crystals produced by *M. parvus OBBP*. Calcium carbonate precipitation was further confirmed from XRD, TEM, and SEM analyses (Fig. 2, Fig. 3, Fig. 4). The three possible calcium carbonate crystal polymorphs (i.e., calcite, vaterite, aragonite) were observed in the *M. parvus* OBBP cultures in 5 g liter^{-1} of calcium formate. Thermodynamically, vaterite and aragonite are metastable crystal phases, whereas calcite is the more stable polymorph (40). Vaterite, commonly formed at a high supersaturation, was suggested to be the precursor of calcite, which is formed at a low supersaturation (41, 42). In our study, vaterite seemed to be the main crystal phase at most incubation type. The type of calcium carbonate polymorphs is important for biotechnological applications in the construction industry. Calcite is the most preferred crystal phase due to its stability and its higher consolidating effect (41). However, vaterite is not a disadvantage as it could also be stabilized in the longer term (43).

From the EDS spectra analyses, it could be confirmed that the spherulite crystal in SEM images were composed mostly of calcium carbonate. The spherulite crystal observed from SEM analyses is known to be the final morphological stage of the biogenic calcium carbonate crystal development (28, 31). However, in contrast to a previous study (31), the grouped spherulite crystals were formed at a high salinity (i.e., 10 g liter^{-1} of calcium formate) instead of at low salinity. The lower EDS peaks from calcium carbonate crystals spots compared to the pure calcium carbonate might indicate that the biogenic crystal was lower in purity. This could be due to the incorporation of an organic matrix, such as the cell debris, in the crystal. Moreover, although the exact role of bacterial cell in MICP is still debatable (1), SEM and TEM analyses indicate that bacteria could act as the nucleation site for the crystals (3). Previously, it was hypothesized that the bacterial cell wall provide a template for the calcium carbonate crystal formation (44). The cell wall, consisting of different functional groups (e.g., hydroxyl, carboxyl), binds calcium ions and further react with the carbonate ions to form calcium carbonate (41).

This study presents the first report of calcium carbonate precipitation from calcium formate, using *M. parvus* OBBP culture; furthermore, the optimum precipitate yields from different culture densities and calcium formate concentrations in grown *M. parvus* OBBP culture were described. For biotechnological purposes, this process has several advantages compared to urea based biogenic precipitation. Because MICP from calcium formate would not release ammonia to the air nor produce nitric acid as by-product, when applied on building materials, less pollution would impact the environment and the biodeterioration risk of the material would be decreased. In addition, MOB could also remove methane, a greenhouse gas, adding further functionality to the building material. In the construction industry, the formate oxidation-driven MICP could be used to improve the durability of concrete by means of surface treatment (8) or to conserve stone-based buildings or historical monuments from deteriorating by

consolidation the stone (12, 45, 46). For all of these applications, replacing the currently applied urea-based MICP as the basis of the process would represent a significant improvement toward an environmental sustainable approach.

For future studies, the process needs to be applied on building materials. It should be determined if the calcium carbonate deposition on the material's surface could sufficiently protect the material from deterioration or ingression of deleterious substances. Comparison should also be made to the performance of the biological surface treatment on building materials using the urea-based approach.

ACKNOWLEDGMENTS

The project was fully funded by the SIM-SHE SECEMIN project (SIM 2009-1) and the Geconcerteerde Onderzoeksactie of Ghent University (BOF09/GOA/005).

We thank Colin Murrell for providing the bacterial strain. We also thank Joachim Desloover and Emma Hernandez-Sanabria for critically reviewing the manuscript.

REFERENCES

1. **De Muynck W, De Belie N, Verstraete W.** 2010. Microbial carbonate precipitation in construction materials: a review. Ecol. Eng. **36:**118–136. http://dx.doi.org/10.1016/j.ecoleng.2009.02.006.
2. **Castanier S, Le Metayer-Levrel G, Perthuisot JP.** 1999. Ca-carbonates precipitation and limestone genesis: the microbiogeologist point of view. Sediment Geol. **126:**9–23. http://dx.doi.org/10.1016/S0037-0738(99)00028-7.
3. **Hammes F, Verstraete W.** 2002. Key roles of pH and calcium metabolism in microbial carbonate precipitation. Rev. Environ. Sci. Biotechnol. **1:**3–7. http://dx.doi.org/10.1023/A:1015135629155.
4. **Braissant O, Verrecchia EP, Aragno M.** 2002. Is the contribution of bacteria to terrestrial carbon budget greatly underestimated? Naturwissenschaften **89:**366–370. http://dx.doi.org/10.1007/s00114-002-0340-0.
5. **Cacchio P, Ercole C, Cappuccio G, Lepidi A.** 2003. Calcium carbonate precipitation by bacterial strains isolated from a limestone cave and from a loamy soil. Geomicrobiol. J. **20:**85–98. http://dx.doi.org/10.1080/01490450303883.
6. **Morita RY.** 1980. Calcite precipitation by marine bacteria. Geomicrobiol. J. **2:**63–82. http://dx.doi.org/10.1080/01490458009377751.
7. **Thompson JB, Ferris FG.** 1990. Cyanobacterial precipitation of gypsum calcite, and magnesite from natural alkaline lake water. Geology **18:**995–998. http://dx.doi.org/10.1130/0091-7613(1990)018<0995:CPOGCA>2.3.CO;2.
8. **De Muynck W, Cox K, De Belle N, Verstraete W.** 2008. Bacterial carbonate precipitation as an alternative surface treatment for concrete. Constr. Build. Mater. **22:**875–885. http://dx.doi.org/10.1016/j.conbuildmat.2006.12.011.
9. **Wang JY, De Belie N, Verstraete W.** 2012. Diatomaceous earth as a protective vehicle for bacteria applied for self-healing concrete. J. Ind. Microbiol. Biotechnol. **39:**567–577. http://dx.doi.org/10.1007/s10295-011-1037-1.
10. **Van Tittelboom K, De Belie N, De Muynck W, Verstraete W.** 2010. Use of bacteria to repair cracks in concrete. Cem. Concr. Res. **40:**157–166. http://dx.doi.org/10.1016/j.cemconres.2009.08.025.
11. **Stocks-Fischer S, Galinat JK, Bang SS.** 1999. Microbiological precipitation of $CaCO_3$. Soil Biol. Biochem. **31:**1563–1571. http://dx.doi.org/10.1016/S0038-0717(99)00082-6.
12. **Dick J, De Windt W, De Graef B, Saveyn H, Van der Meeren P, De Belie N, Verstraete W.** 2006. Bio-deposition of a calcium carbonate layer on degraded limestone by *Bacillus* species. Biodegradation **17:**357–367. http://dx.doi.org/10.1007/s10532-005-9006-x.
13. **Bates RG, Pinching GD.** 1949. Acidic dissociation constant of ammonium Ion at 0° to 50° C, and the base strength of ammonia. J. Res. Nat. Bur. Stand. **42:**419–430. http://dx.doi.org/10.6028/jres.042.037.
14. **Piqué F, Dei L, Ferroni E.** 1992. Physicochemical aspects of the deliquescence of calcium nitrate and its implications for wall painting conservation. Stud. Conserv. **37:**217–227. http://dx.doi.org/10.1179/sic.1992.37.4.217.
15. **Hanson RS, Hanson TE.** 1996. Methanotrophic bacteria. Microbiol. Rev. **60:**439–471.
16. **Pieja AJ, Sundstrom ER, Criddle CS.** 2011. Poly-3-hydroxybutyrate metabolism in the type II methanotroph *Methylocystis parvus* OBBP. Appl. Environ. Microbiol. **77:**6012–6019. http://dx.doi.org/10.1128/AEM.00509-11.
17. **Pieja AJ, Rostkowski KH, Criddle CS.** 2011. Distribution and selection of poly-3-hydroxybutyrate production capacity in methanotrophic proteobacteria. Microb. Ecol. **62:**564–573. http://dx.doi.org/10.1007/s00248-011-9873-0.
18. **Ho A, Kerckhof FM, Luke C, Reim A, Krause S, Boon N, Bodelier LEP.** 2012. Conceptualizing functional traits and ecological characteristics of methane-oxidizing bacteria as life strategies. Environ. Microbiol. Rep. **5:**335–345. http://dx.doi.org/10.1111/j.1758-2229.2012.00370.x.
19. **Semrau JD, DiSpirito AA, Yoon S.** 2010. Methanotrophs and copper. FEMS Microbiol. Rev. **34:**496–531. http://dx.doi.org/10.1111/j.1574-6976.2010.00212.x.
20. **Whittenbury R, Phillips KC, Wilkinson JF.** 1970. Enrichment, isolation and some properties of methane-utilizing bacteria. J. Gen. Microbiol. **61:**205–218. http://dx.doi.org/10.1099/00221287-61-2-205.
21. **Van Nevel S, Koetzsch S, Weilenmann H-U, Boon N, Hammes F.** 2013. Routine bacterial analysis with automated flow cytometry. J. Microbiol. Methods **94:**73–76. http://dx.doi.org/10.1016/j.mimet.2013.05.007.
22. **De Roy K, Clement L, Thas O, Wang Y, Boon N.** 2012. Flow cytometry for fast microbial community fingerprinting. Water Res. **46:**907–919. http://dx.doi.org/10.1016/j.watres.2011.11.076.
23. **Hosseinkhani B, Sobjerg LS, Rotaru A-E, Emtiazi G, Skrydstrup T, Meyer RL.** 2012. Microbially supported synthesis of catalytically active bimetallic Pd-Au nanoparticles. Biotechnol. Bioeng. **109:**45–52. http://dx.doi.org/10.1002/bit.23293.
24. **Asenjo JA, Suk JS.** 1986. Microbial conversion of methane into poly-β-hydroxybutyrate (PHB): growth and intracellular product accumulation in a type-II methanotroph. J. Ferment. Technol. **64:**271–278. http://dx.doi.org/10.1016/0385-6380(86)90118-4.
25. **Tijhuis L, Vanloosdrecht MCM, Heijnen JJ.** 1993. A thermodynamically based correlation for maintenance Gibbs energy-requirements in aerobic and anaerobic chemotropic growth. Biotechnol. Bioeng. **42:**509–519. http://dx.doi.org/10.1002/bit.260420415.
26. **Knief C, Dunfield PF.** 2005. Response and adaptation of different methanotrophic bacteria to low methane mixing ratios. Environ. Microbiol. **7:**1307–1317. http://dx.doi.org/10.1111/j.1462-2920.2005.00814.x.
27. **Schnell S, King GM.** 1996. Responses of methanotrophic activity in soils and cultures to water stress. Appl. Environ. Microbiol. **62:**3203–3209.
28. **Braissant O, Cailleau G, Dupraz C, Verrecchia AP.** 2003. Bacterially induced mineralization of calcium carbonate in terrestrial environments: the role of exopolysaccharides and amino acids. J. Sediment. Res. **73:**485–490. http://dx.doi.org/10.1306/111302730485.
29. **Martin G, Guggiari M, Bravo D, Zopfi J, Cailleau G, Aragno M, Job D, Verrecchia E, Junier P.** 2012. Fungi, bacteria, and soil pH: the oxalate-carbonate pathway as a model for metabolic interaction. Environ. Microbiol. **14:**2960–2970. http://dx.doi.org/10.1111/j.1462-2920.2012.02862.x.
30. **Mucci A.** 1983. The solubility of calcite and aragonite in seawater at various salinities, temperatures, and one atmosphere total pressure. Am. J. Sci. **283:**780–799. http://dx.doi.org/10.2475/ajs.283.7.780.
31. **Rivadeneyra MA, Parraga J, Delgado R, Ramos-Cormenzana A, Delgado G.** 2004. Biomineralization of carbonates by *Halobacillus trueperi* in solid and liquid media with different salinities. FEMS Microbiol. Ecol. **48:**39–46. http://dx.doi.org/10.1016/j.femsec.2003.12.008.
32. **Ho A, Lueke C, Frenzel P.** 2011. Recovery of methanotrophs from disturbance: population dynamics, evenness and functioning. ISME J. **5:**750–758. http://dx.doi.org/10.1038/ismej.2010.163.
33. **Ho A, Frenzel P.** 2012. Heat stress and methane-oxidizing bacteria: effects on activity and population dynamics. Soil Biol. Biochem. **50:**22–25. http://dx.doi.org/10.1016/j.soilbio.2012.02.023.
34. **De Muynck W, Verbeken K, De Belie N, Verstraete W.** 2010. Influence of urea and calcium dosage on the effectiveness of bacterially induced carbonate precipitation on limestone. Ecol. Eng. **36:**99–111. http://dx.doi.org/10.1016/j.ecoleng.2009.03.025.
35. **Mahanty B, Kim S, Kim CG.** 2013. Assessment of a biostimulated or bioaugmented calcification system with *Bacillus pasteurii* in a simulated soil environment. Microb. Ecol. **65:**679–688. http://dx.doi.org/10.1007/s00248-012-0137-4.
36. **Mahanty B, Kim S, Kim CG.** 2013. Biocalcification mediated reduction

of PAHs bioavailability in artificially contaminated soil. Water Air Soil Pollut. **224:**1479. http://dx.doi.org/10.1007/s11270-013-1479-3.
37. **Hammes F, Boon N, de Villiers J, Verstraete W, Siciliano SD.** 2003. Strain-specific ureolytic microbial calcium carbonate precipitation. Appl. Environ. Microbiol. **69:**4901–4909. http://dx.doi.org/10.1128/AEM.69.8.4901-4909.2003.
38. **De Belie N.** 2010. Microorganisms versus stony materials: a love-hate relationship. Materials Struct. **43:**1191–1202. http://dx.doi.org/10.1617/s11527-010-9654-0.
39. **Jonkers HM, Thijssen A, Muyzer G, Copuroglu O, Schlangen E.** 2010. Application of bacteria as self-healing agent for the development of sustainable concrete. Ecol. Eng. **36:**230–235. http://dx.doi.org/10.1016/j.ecoleng.2008.12.036.
40. **Spanos N, Koutsoukos PG.** 1998. The transformation of vaterite to calcite: effect of the conditions of the solutions in contact with the mineral phase. J. Crystal Growth **191:**783–790. http://dx.doi.org/10.1016/S0022-0248(98)00385-6.
41. **Rodriguez-Navarro C, Rodriguez-Gallego M, Ben Chekroun K, Gonzalez-Munoz MT.** 2003. Conservation of ornamental stone by *Myxococcus xanthus*-induced carbonate biomineralization. Appl. Environ. Microbiol. **69:**2182–2193. http://dx.doi.org/10.1128/AEM.69.4.2182-2193.2003.
42. **Jimenez-Lopez C, Jroundi F, Pascolini C, Rodriguez-Navarro C, Pinar-Larrubia G, Rodriguez-Gallego M, Gonzalez-Munoz MT.** 2008. Consolidation of quarry calcarenite by calcium carbonate precipitation induced by bacteria activated among the microbiota inhabiting the stone. Int. Biodeterior. Biodegrad. **62:**352–363. http://dx.doi.org/10.1016/j.ibiod.2008.03.002.
43. **Rodriguez-Navarro C, Jimenez-Lopez C, Rodriguez-Navarro A, Gonzalez-Munoz MT, Rodriguez-Gallego M.** 2007. Bacterially mediated mineralization of vaterite. Geochim. Cosmochim. Acta **71:**1197–1213. http://dx.doi.org/10.1016/j.gca.2006.11.031.
44. **Ferris FG, Fyfe WS, Beveridge TJ.** 1987. Bacteria as nucleation sites for authigenic minerals in a metal-contaminated lake sediment. Chem. Geol. **63:**225–232. http://dx.doi.org/10.1016/0009-2541(87)90165-3.
45. **De Muynck W, Verbeken K, De Belie N, Verstraete W.** 2013. Influence of temperature on the effectiveness of a biogenic carbonate surface treatment for limestone conservation. Appl. Microbiol. Biotechnol. **97:**1335–1347. http://dx.doi.org/10.1007/s00253-012-3997-0.
46. **Dhami NK, Reddy MS, Mukherjee A.** 2013. *Bacillus* megaterium mediated mineralization of calcium carbonate as biogenic surface treatment of green building materials. World J. Microbiol. Biotechnol. **29:**2397–2406. http://dx.doi.org/10.1007/s11274-013-1408-z.
47. **Warren LA, Maurice PA, Parmar N, Ferris FG.** 2001. Microbially mediated calcium carbonate precipitation: implications for interpreting calcite precipitation and for solid-phase capture of inorganic contaminants. Geomicrobiol. J. **18:**93–115. http://dx.doi.org/10.1080/01490450151079833.
48. **Mitchell AC, Ferris FG.** 2006. The Influence of *Bacillus pasteurii* on the nucleation and growth of calcium carbonate. Geomicrobiol. J. **23:**213–226. http://dx.doi.org/10.1080/01490450600724233.
49. **Dupraz S, Menez B, Gouze P, Leprovost R, Benezeth P, Pokrovsky OS, Guyot F.** 2009. Experimental approach of CO_2 biomineralization in deep saline aquifers. Chem. Geol. **265:**54–62. http://dx.doi.org/10.1016/j.chemgeo.2008.12.012.
50. **Dupraz S, Parmentier M, Menez B, Guyot F.** 2009. Experimental and numerical modeling of bacterially induced pH increase and calcite precipitation in saline aquifers. Chem. Geol. **265:**44–53. http://dx.doi.org/10.1016/j.chemgeo.2009.05.003.
51. **Chou C-W, Seagren EA, Aydilek AH, Lai M.** 2011. Biocalcification of sand through ureolysis. J. Geotech. Geoenviron. Eng. **137:**1179–1189. http://dx.doi.org/10.1061/(ASCE)GT.1943-5606.0000532.
52. **Bachmeier KL, Williams AE, Warmington JR, Bang SS.** 2002. Urease activity in microbiologically induced calcite precipitation. J. Biotechnol. **93:**171–181. http://dx.doi.org/10.1016/S0168-1656(01)00393-5.
53. **Lee J, Kim CG, Mahanty B.** 2014. Mineralization of gaseous CO_2 by *Bacillus megaterium* in close environment system. Water Air Soil Pollut. **225:**1787. http://dx.doi.org/10.1007/s11270-013-1787-7.
54. **Achal V, Pan XL.** 2011. Characterization of urease and carbonic anhydrase producing bacteria and their role in calcite precipitation. Curr. Microbiol. **62:**894–902. http://dx.doi.org/10.1007/s00284-010-9801-4.
55. **Ghashghaei S, Emtiazi G.** 2013. Production of calcite nanocrystal by a urease-positive strain of *Enterobacter ludwigii* and study of its structure by SEM. Curr. Microbiol. **67:**406–413. http://dx.doi.org/10.1007/s00284-013-0379-5.
56. **Nemati M, Greene EA, Voordouw G.** 2005. Permeability profile modification using bacterially formed calcium carbonate: comparison with enzymic option. Process Biochem. **40:**925–933. http://dx.doi.org/10.1016/j.procbio.2004.02.019.
57. **Park SJ, Park YM, Chun WY, Kim WJ, Ghim SY.** 2010. Calcite-forming bacteria for compressive strength improvement in mortar. J. Microbiol. Biotechnol. **20:**782–788.
58. **Achal V, Pan X, Fu Q, Zhang D.** 2012. Biomineralization based remediation of As(III) contaminated soil by *Sporosarcina ginsengisoli*. J. Hazard. Mater. **201:**178–184. http://dx.doi.org/10.1016/j.jhazmat.2011.11.067.
59. **Achal V, Pan XL, Zhang DY.** 2011. Remediation of copper-contaminated soil by *Kocuria flava* CR1, based on microbially induced calcite precipitation. Ecol. Eng. **37:**1601–1605. http://dx.doi.org/10.1016/j.ecoleng.2011.06.008.
60. **Achal V, Pan XL, Zhang DY, Fu QL.** 2012. Bioremediation of Pb-contaminated soil based on microbially induced calcite precipitation. J. Microbiol. Biotechnol. **22:**244–247. http://dx.doi.org/10.4014/jmb.1108.08033.